Xenon postconditioning attenuates neuronal injury after spinal cord ischemia/reperfusion injury by targeting endoplasmic reticulum stress- associated apoptosis

Lan Luo
Department of Anesthesiology, Capital Medical University Affiliated Beijing Friendship Hospital
Yuqing Wang
Tsinghua Laboratory of Brain and Intelligence, Tsinghua University
Jiaqi Tong
Department of Anesthesiology, Capital Medical University Affiliated Beijing Friendship Hospital
Lu Li
Department of Anesthesiology, Capital Medical University Affiliated Beijing Friendship Hospital
Yanbing Zhu
Beijing Clinical Research Institute, Capital Medical University Affiliated Beijing Friendship Hospital
Mu Jin (jinmu0119@hotmail.com)
Department of Anesthesiology, Capital Medical University Affiliated Beijing Friendship Hospital

Research Article

Keywords: spinal cord ischemia/reperfusion injury, xenon, endoplasmic reticulum stress, neuron, apoptosis

Posted Date: May 2nd, 2023

DOI: https://doi.org/10.21203/rs.3.rs-2853195/v1

Version of Record: A version of this preprint was published at Neurosurgical Review on August 29th, 2023. See the published version at https://doi.org/10.1007/s10143-023-02125-x.

Abstract

Purpose: To explore the underlying mechanisms of xenon (Xe) protect against spinal cord ischemia/reperfusion injury (SCIRI).

Materials and methods: A SCIRI rat model was induced by abdominal artery occlusion for 85 min and reperfusion. Xe postconditioning (50% Xe) was administered 1 h after 1 h of reperfusion. At reperfusion time points (2, 4, 6, and 24 h), rats were treated with spinal cord scans by MRI to assess the time of peak spinal cord injury after SCIRI. Subsequently, endoplasmic reticulum (ER) stress inhibitor sodium 4-phenylbutyrate (4-PBA) was administered by daily intraperitoneal injection (50 mg/kg) for 5 days before SCIRI. At 4 hours after reperfusion, motor function, immunofluorescence staining, hematoxylin and eosin (HE) staining, Nissl staining, TUNEL staining, real-time reverse transcription polymerase chain (RT-PCR) reaction, and Western blot analyses were performed to investigate the protective effects of Xe against SCIRI.

Results: In the rat I/R model, spinal cord edema peaked at reperfusion 4 h. SCIRI activated ER stress, which was located in neurons. Xe postconditioning remarkably alleviated hind limb motor function, reduced neuronal apoptosis rate, increased the number of normal neurons, inhibited the expression of ER stress related protein in spinal cord. Furthermore, administration of the ER stress inhibitor 4-PBA strongly decreased ER stress-induced apoptosis following SCIRI.

Conclusions: Xe postconditioning inhibits ER stress activation, which contributes to alleviate SCIRI by suppressing neuronal apoptosis.

Introduction

Spinal cord ischemia/reperfusion injury (SCIRI) is the secondary damage of primary spinal cord injury, which is the most devastating complication in clinical thoracoabdominal aneurysm repair[1, 2]. Due to segmental blood supply and relatively poor collateral circulation, the spinal cord is prone to IRI. SCIRI can induce neural dysfunction, paralysis and paraplegia, eventually causing adverse effects to the patients both mentally and physically[3, 4]. Unfortunately, although considerable therapeutic interventions have been proposed to alleviate the damage of neurological function after SCIRI, the overall effect is limited[5]. In SCIRI, nerve cells are vulnerable to ischemic injury due to their high demand for energy, and the damage of nerve cells is an important reason for their slow recovery of patients. Moreover, neuronal damage is associated with lower limb motor dysfunction, and it is challenging to repair nerve function after SCIRI[6, 7]. Neuronal apoptosis has a crucial effect on the loss of behavioral and sensory function of SCIRI[8]. Therefore, it is crucial to explore the specific molecular pathway mediating apoptosis in order to design an effective therapy for SCIRI.

In recent years, increasing literature has reported that endoplasmic reticulum (ER) stress is involved in the occurrence of SCIRI[9]. Glucose-regulated protein 78/immunoglobulin heavy chain-binding protein (GRP78/BIP) is a marker protein of ER stress. Under physiological conditions, GRP78 combines with three

ER transmembrane proteins, protein kinase R-like ER kinase (PERK), inositol-requiring enzyme 1 (IRE1), and activating transcription factor 6 (ATF6), in an inactive state[10]. The downstream protein of ER stress, C/EBP homologous protein (CHOP), is an apoptotic transcription factor that is induced in response to ER stress[11]. CHOP can lead to the cell apoptosis by activating caspase-3, which is a regulator of caspase-dependent apoptosis[12]. Accumulated evidence also shows that CHOP is a critical mediator responsible for ER stress-induced apoptosis[13]. Mild SCIRI may lead to induction of the unfolded protein response (UPR) in the ER. However, persistent ER stress activates the ER stress-related apoptosis pathway, which ultimately aggravates SCIRI[14].

Xenon (Xe) has been considered an ideal anesthetic that is used medically as a general anesthetic and in magnetic resonance imaging (MRI)[15]. Xe has been recognized for its hemodynamic stability, decreased analgesic requirement, lower blood levels of catecholamines, and better regional organ perfusion[16]. Xe is a pleiotropic drug with actions at a variety of targets implicated in the secondary injury cascade including N-methyl-D-aspartate receptors[17], potassium channels[18], activation of hypoxia inducible 1 alpha[19], and an increase in erythropoietin levels[20]. Xe has neuroprotective properties for its use in anesthesia to attenuate neuronal injury, neurocognitive, and neurological dysfunction. Moreover, Xe significantly alleviates SCIRI[21, 22]. However, the specific mechanism by which this occurs has not yet been elucidated. Consequently, it is necessary to explore the molecular mechanism of Xe postconditioning against SCIRI in rats.

In this study, we elucidated the relationship between ER stress and apoptosis in the context of neuronal damage of SCIRI.

Materials And Methods

This study consisted of three experiments (experiments one–three). In experiment 1, we assessed the time of peak spinal cord injury after SCIRI by MRI. Experiment 2 was conducted to investigate ER stress activation and the relationship between ER stress and neurons after SCIRI. To elucidate the neuroprotective effects of Xe, we used 4-phenlybutyric acid (4-PBA) to gain insights into the mechanisms of the protective effects in experiment 3, which was designed to reveal the association of Xe inhalation during reperfusion with ER stress-induced apoptosis

Animals

Adult male Sprague-Dawley rats weighing 250–300 g were used. The rats were maintained in a pathogen-free, temperature-controlled environment under a 12 h light/dark cycle at Beijing Friendship Hospital. The experimental procedures were approved by the Institutional Animal Care and Use Committee of Beijing Friendship Hospital and maintained in accordance with the Regulations for the Administration of Affairs Concerning Experimental Animals regarding the care and use of laboratory animals.

SCIRI

The SCIRI model was established according to the Zivin method[23]. Briefly, after 12 h-fasting, the rats underwent the following procedures. All rats were anesthetized by intraperitoneal injection of 4% sodium pentobarbital (50 mg/kg) before surgery and endotracheally intubated (16 g trocar sleeve). Breathing was controlled using a ventilator (tidal volume 15 mL/Kg, breathing frequency 80–130 times/min, breathing ratio 1:1)[24] with body temperature kept under light. The abdominal cavity was exposed to the abdominal aorta in strict accordance with aseptic procedures. The intestine was wrapped with wet gauze to fully expose the abdominal aorta and inferior vena cava, which were gently separated by forceps. Next, the abdominal aorta was clamped between the left and right renal arteries with a non-invasive artery clamp, and it was confirmed that the abdominal aorta pulsation disappeared after the arterial clip disappeared. After clamping for 85 min, the arterial clamp was removed, and the distal reperfusion was visually observed. After ensuring that no bleeding or damage occurred, the peritoneal cavity was closed. In the Sham group without ischemia, the abdomen was opened to expose the abdominal aorta, but without clamping. The body temperature of rats was kept constant throughout the procedure. Rats were maintained in standard cages with free access to food and water.

Xe treatment

As mentioned in a previous study[21], we prepared a premixed gas (50% nitrogen and 50% Xe). Oxygen and premixed gas were blended and supplied to the animals through the small animal ventilator (Shanghai, China). After 1 h of reperfusion, the rats in the Xe postconditioning group inhaled 50 vol% Xe and 50 vol% oxygen for 1 h, whereas the other group of rats inhaled 50 vol% nitrogen and 50 vol% oxygen for 1 h after 1 h of reperfusion.

Experimental protocol

Experiment one

The rats were randomly divided into three groups: Sham, I/R, and I/R + Xe groups. According to reperfusion time points (2h, 4h, 6h, and 24 h), three rats at each time point (12 rats) were treated with spinal cord scans on the 7.0 T MRI system (BioSpec 70/20; Bruker, Germany) (Fig. 1A). Anesthesia was induced with 4% isoflurane (RWD Life Science, USA) and maintained during surgery using 2% isoflurane supplemented with regular air. The body temperature was kept at 37°C through the circulating water tank, and the respiratory status was monitored in real time through the encoder receiver transmitter module. The spinal edema imaging sequence was the T2_TurboRARE sequence.

Experiment two

The other 30 animals (Sham, I/R, and Xe groups; n = 10, each) were anesthetized and underwent the same surgical procedures as described in experiment one. At 4 h after the reperfusion, five rats in each subgroup were euthanized to obtain lumbar spinal cord tissue (L3–5), which was fixed in 4% paraformaldehyde, embedded in paraffin, and cut into spinal cord sections for immunofluorescence

staining. Lumbar spinal cord tissue was immediately collected from the other five rats in each group and was stored at -80°C until western blot analysis (Fig. 2A).

Experiment three

To better explain the possible protective mechanisms of Xe on SCIRI, we added the ER stress inhibitor 4-PBA. Fifty new rats were randomly assigned to Sham, I/R, I/R+Xe (Xe), I/R+4-PBA, and I/R+Xe+4-PBA (Xe+4-PBA) groups (n = 10 each) (Figure 4A). I/R+4-PBA and Xe+4-PBA groups were intraperitoneally (i.p.) injected with 4-PBA (50 mg/kg/d, Sigma-Aldrich, USA) for 5 d before SCRI[25, 26]. The other groups were intraperitoneally injected with an equivalent volume of vehicle for the same duration. Second, rats were euthanized with a lethal dose of anesthesia at 4 h after reperfusion and after a final neurological functional assessment. Subsequently, sample collection was the same as experiment two for hematoxylin and eosin (H&E) staining, Nissl staining, terminal deoxynucleotidyl transferase dUTP nick end labeling (TUNEL) staining, western blot analyses, and real-time reverse transcription polymerase chain (RT-PCR) detection.

Neurological assessment

The ability of rats to use their hindlimbs was investigated by an assessor blinded to the experimental protocol with the Basso, Beattie and Bresnahan (BBB) scale[26] and Tarlov[23] scoring system over 3 min on postreperfusion for 4 h.

H&E staining

After fixing in paraformaldehyde and dehydration with alcohol, the spinal cord L3–5 specimens were embedded with paraffin and sectioned into 5 μm segments with a microtome. The spinal cord sections were deparaffinized in xylene, rehydrated in graded ethanol, and stained with H&E. After mounting with neutral balsam, slices were observed under a light microscope at 20× magnification (Leica, Germany).

Nissl staining

Deparaffinized spinal cord tissues of 5 μm thickness were stained with 0.5% thionine (Solarbio, China) for 15 min at room temperature and differentiated in 0.25% acetate ethanol for seconds. After dehydrating with ethanol and xylene, slices were observed under a Leica light microscope at 20× magnification (Leica). The total number of normal motor neurons in half of the anterior horns of each section was counted in five random fields (40×) using a light microscope.

Immunofluorescence staining

The spinal cord sections were deparaffinized in xylene and rehydrated with graded ethanol solutions. Then the slices were placed in a boiling EDTA buffer (pH 9.0) for 20 min for microwave antigen retrieval. After washing twice with phosphate-buffered saline, the sections were permeabilized in 0.3% Triton X-100 (Solarbio) for 15 min, blocked in normal goat serum (Solarbio) at room temperature for 1 h, and

incubated with neuronal nuclear protein (NeuN, 1:100, Abcam, USA), GRP78 (1:100, Abcam) at 4°C overnight. Then the sections were incubated with secondary antibodies conjugated with Alexa Fluor 488 (1:200, Abcam) and Alexa Fluor 594 (1:200, Abcam) for 2 h at room temperature. Finally, sections were observed blindly under laser scanning confocal microscope (Olympus, Japan). Immune-positive cells from five randomly selected fields were counted under a confocal microscope at 40× magnification by experimenters that were blinded to the experimental group.

TUNEL staining

The slides with the spinal cord tissue were incubated with proteinase K (Beyotime Biotechnology, China) for 30 min at 37°C, after which they were processed with the In Situ Cell Death Detection Kit according to the manufacturer's instructions (Beyotime). 3,3'-Diaminobenzidine was used for staining. Finally, the sections were dehydrated, cleared, and mounted according to the procedure described in the Nissl staining section. Next, TUNEL-positive cells (brown) were counted, and the apoptosis rate was calculated and expressed as the percentage of TUNEL-positive cells. Cell counting was performed using high optical microscopy by a histologist blinded to the groups.

Western blot analysis

Spinal cord was harvested 4 h after SCIRI. Total proteins were extracted with M-PER Mammalian Protein Extraction Reagent (Thermo, USA). The following primary antibodies: GRP78 (1:1000), IRE1α (1:1000, Cell Signaling Technology (CST), USA), ATF6 (1:1000, Abcam), PERK (1:1000, Abcam), CHOP (1:1000, CST), B-cell lymphoma 2 (Bcl-2, 1:3000, Abcam), Bcl-2-associated X, apoptosis regulator (Bax, 1:3000, Abcam), caspase-3 (1:2000, Abcam), and β-actin (1:2500, Abcam). Blots were exposed to the Molecular Imager (ChemiDo XRS+; Bio-Rad, Hercules, USA) and analyzed with ImageJ software (Scion Co., Walkersville, USA).

RNA isolation and quantification

Total RNA from L3–5 spinal cords was extracted using TRIZOL reagent (Sigma) following the manufacturer's protocol. The PrimeScript™ RT reagent kit (Takara, Tokyo, Japan) was used to reverse transcribe total RNA into cDNA. cDNA was incubated with SYBR Green Master Mix (Yeasen) and the reaction was run on the Prism 7500 Fast Real-Time PCR System (Applied Biosystems, Waltham, USA) with the corresponding primers. The $2^{-\Delta\Delta Ct}$ method was used to calculate the RNA expression. β-actin was used as the internal control. The primers are listed in Table 1.

Statistical analyses

All statistical analyses were carried out using SPSS statistical software (version 26.0; IBM, USA). All data were expressed as mean ± standard deviation. One-way analysis of variance followed by Least Significance Difference post hoc test was used to measure differences between mean values of the different treated groups. $P < 0.05$ was considered statistically significant.

Results

The degree of spinal cord edema peaks at reperfusion 4 h after SCIRI

IRI is defined as restored blood flow to ischemic tissue or organs, which exacerbates tissue injury. Subsequently, a common and serious secondary injury is observed clinically. Through spinal cord MRI, we found that SCIRI can result in lumbar spinal cord edema, with the most severe effect occurring at 4 h after reperfusion. Furthermore, Xe postconditioning can effectively mitigate spinal cord edema (Fig. 1B-C) and relieve IRI.

Xe postconditioning inhibits the activation of ER stress after SCIRI

Based on the MRI results, the spinal cord was collected at 4 h after reperfusion. The expression of ER stress-related factors in the spinal cord of SCRI rats was detected by western blot analysis (Fig. 2B). The results showed that the expression level of GRP78 in the I/R group was significantly increased compared with the Sham group ($P < 0.05$). Moreover, SCIRI increased the expression of ER stress-related proteins IRE1α, PERK, and ATF6 compared to the Sham group ($P < 0.05$). Compared to the I/R group, Xe postconditioning significantly lowered GRP78, ATF6, and PERK protein expression ($P < 0.05$), but IRE1α expression in the Xe and I/R groups was similar (Fig. 2C-F).

GRP78 expression in neurons after SCIRI

To confirm our hypothesis, we detected the localization of ER stress marker GRP78 in the L3–5 spinal cord tissue with immunofluorescence at 4 h after injury. The immunofluorescence labeling of GRP78 in the gray matter is shown in Figure 3. Similar to the protein levels detected by western blotting, GRP78-positive fluorescence labeling increased in the I/R group in contrast to that in the Sham group, which confirmed that the ER stress in the spinal cord tissue is activated in IRI. Simultaneously, we double-labeled the GRP78 with neuronal nuclei marker NeuN in the spinal cord tissue (Fig. 3). The representative higher magnification images show GRP78 around the neuronal nuclei, indicating that ER stress occurred in neuronal cells.

Xe postconditioning alleviates hindlimb function after SCIRI

As shown in Fig. 4B to 4C, according to the BBB and Tarlov measurements, SCIRI induced severe neurological deficits of lower extremities. Xe postconditioning significantly improved neurological dysfunction ($P < 0.05$ vs. the I/R group), indicating that Xe is beneficial to the recovery of hindlimb locomotor function in rats with SCIRI. Furthermore, hindlimb locomotor function after SCIRI were markedly ameliorated by 4-PBA treatment ($P < 0.05$)

Xe postconditioning attenuates morphological changes and neuronal apoptosis after SCIRI

As shown in Fig. 4F, the H&E-stained rat spinal cord tissues showed a normal neuron morphology in the Sham group. Furthermore, neutrophile granulocyte infiltration was revealed in the I/R group, whereas

more intact motor neurons with a fine granular cytoplasm were observed in the Xe group. Normal neurons contained Nissl bodies in the cytoplasm, with loose chromatin and prominent nucleoli; however, the damaged neurons contained relatively few Nissl bodies and had dark and shrunken nucleoli. The results of Nissl staining demonstrated that the number of Nissl bodies was markedly decreased after SCIRI ($P < 0.05$), but Xe postconditioning greatly alleviated neuronal injury, exhibited by increased number of Nissl bodies (Fig. 4D; $P < 0.05$). Interestingly, treatment with the ER stress inhibitor 4-PBA significantly attenuated the number of normal neurons after SCIRI (Fig. 4D; $P < 0.05$ vs. the I/R group).

In addition, the TUNEL-stained rat spinal cord tissues indicated significantly higher neural cell apoptosis rates in the SCIRI model and Xe groups than in the Sham group (Fig. 4F). Moreover, neural cell apoptosis rate was significantly lower in the Xe group than in the I/R group, indicating that Xe postconditioning prevented SCIRI-induced neural cell apoptosis in the rat spinal cord (Fig. 4E; $P < 0.05$). Importantly, neural cell apoptosis rate was significantly higher in the I/R+4-PBA group than in the Xe group (Fig. 4E; $P < 0.05$).

Xe postconditioning inhibits activation of ER stress after SCIRI

The expression of ER stress-related factors in the spinal cord of SCIRI rats was detected by western blotting (Fig. 5A) and RT-PCR. The results showed that the expression levels of GRP78 in the I/R group were significantly increased compared with the Sham group (Fig. 5B, $P < 0.05$). Moreover, SCIRI increased the expression of ER stress-related proteins IRE1α, PERK, and ATF6 in the I/R group compared to the Sham group (Fig. 5C, D and E, $P < 0.05$). Compared to the I/R group, Xe postconditioning significantly decreased GRP78, ATF6, IRE1α, and PERK protein expression. Furthermore, administration of the ER stress inhibitor 4-PBA strongly suppressed SCIRI-induced ER stress, which resulted in the low expression of GRP78, IRE1α, PERK, and ATF6. In addition, we measured the mRNA expression levels of GRP78, IRE1α, PERK, and ATF6, and the results were consistent with the western blotting results (Fig. 5F and I). These experimental results suggest that ER stress is involved in the pathogenesis of SCIRI, and Xe postconditioning significantly inhibits ER stress.

Xe postconditioning on expression of ER stress-dependent apoptotic proteins after SCIRI

SCIRI apoptosis is a consequence of ER stress, which was examined in the presence of SCIRI with or without Xe treatment. CHOP is classic downstream marker of ER stress that was strongly activated in the spinal cord of rats treated with SCIRI (Fig. 6B). Consistently, SCIRI-induced spinal cord CHOP was also confirmed by RT-PCR (Fig. 6E). However, the high expression of CHOP observed in response to ER stress was notably inhibited in the presence of Xe postconditioning, demonstrating anti-ER stress. Meanwhile, a significant antiapoptotic effect of Xe was also observed, characterized by reduced Bax and caspase-3 levels and enhanced Bcl-2 expression (Fig. 6A, C and D). Meanwhile, Xe postconditioning also enhanced the antiapoptotic effect. This finding was confirmed by decreased mRNA expression of caspase-3 and Bax/Bcl-2(Fig. 6F and G). Expression of caspase-3 and the rate of Bax/Bcl-2 were decreased more significantly with the combination of Xe and 4-PBA compared to 4-PBA alone, and the decrease was greater than with treatment of Xe alone, indicating that Xe postconditioning inhibits ER stress-apoptosis partially by attenuating ER stress.

Discussion

In this study, we found that the degree of spinal cord edema peaked at 4 h after reperfusion. We provided evidence that ER stress is expressed in the spinal cord and participated in SCIRI, which was related to neuronal apoptosis after SCIRI. Furthermore, we observed that Xe postconditioning effectively improved motor functions and prevented nerve cells apoptosis by reversing histological changes in the spinal cord. More importantly, inhibition of ER stress-induced apoptosis was associated with the protective effects of Xe on SCIRI-treated rats.

The pathological mechanism of SCIRI is very complex and has not been entirely elucidated. Many studies have shown that transient ischemia and hypoxia can cause spinal nerve necrosis. The primary mechanisms by which this occurs include free radical and lipid peroxidation, intracellular calcium disruption, release of inflammatory factors, excitatory neurotransmitter damage, apoptosis of nerve cells, and a series of pathophysiological processes[1, 2]. Continual ischemia and hypoxia can aggravate SCIRI, resulting in secondary edema of the spinal cord and increased intrathecal pressure, potentially leading to increased tissue damage and aggravated loss of motor function[6]. Consistent with previous studies, through MRI, we found that spinal cord edema peaked at 4 h after reperfusion. At 4 h, compared to the Sham group, neutrophils infiltrated the spinal cord, the normal neuronal count decreased, and hind limb motor dysfunction occurred in the I/R group. Although diverse pathophysiologic mechanisms of SCIRI have been proposed, it is widely considered that neuronal apoptosis is associated with IRI of the spinal cord[27, 28]. If SCIRI is not treated in time, spinal cord function may incur long-term or permanent damage. Therefore, the importance of exploring effective neuroprotective methods is highlighted, but unfortunately, the mechanism of spinal cord injury caused by SCIRI has not yet been fully elucidated. In recent years, after the discovery of their pharmacologic targets, interest has grown in the use of the noble gases Xe and argon as novel neuroprotectants to minimize or prevent the development of injury after I/R. However, the possible Xe neuroprotective effects and underlying mechanisms in seizure-induced neuronal injury remain unclear. Therefore, our goal was to explore potential signaling pathways on Xe neuroprotective against SCIRI.

Xe is a noble gas, which has been shown to be neuroprotective using in vitro and in vivo models of IRI[29, 30]. Interestingly, previous studies have reported that Xe significantly alleviates SCIRI and cerebral IRI. It reported Xe-delayed postconditioning attenuates SCIRI through activation AKT and extracellular signal-regulated kinase[21]. Previous study reported that delayed Xe postconditioning mitigates SCIRI in rabbits by regulating microglial activation and inflammatory factors[22]. In addition, they also reported that administration of 50% Xe can decrease the apoptosis of nerve cells and get the greatest neuroprotection[31]. Besides, the protective effects of the Xe mixture were verified in C57 neonatal mice including attenuated seizure severity, reduced apoptosis, reduced neuronal injury, and reduced learning and memory defects[32]. Therefore, we investigated the influence of Xe in apoptosis and neuronal injury in SCIRI induced by the ligation of the aorta. In this study, Nissl and TUNEL staining results indicated that, compared with the I/R group, Xe significantly lowered the apoptosis rate (Fig.4E), and finally effectively ameliorated the impairment of locomotor activity according to the BBB scale (Fig. 4B).

ER is the main site responsible for protein synthesis and folding, which serves a vital role in maintaining homeostasis within the cellular microenvironment[33]. Previous studies have shown that under the conditions of SCIRI, the UPR of the ER is induced to react. Persistent ER stress responses induced by the surrounding neuroglia may coordinate damaging inflammatory responses, which help fuel a neurotoxic milieu[34]. Activation of UPR enhances motor recovery after spinal cord injury. The effects of UPR inactivation are associated with a significant increase in the number of damaged axons and reduced amount of oligodendrocytes surrounding the injury zone[35]. During SCI, prolonged ER stress without the cellular protective mechanisms by UPR eventually results in neural apoptosis[36]. In our study, double immunofluorescence staining showed that ER stress occurred in neuronal cells, as indicated by staining with GRP78 (Fig. 3). The results described here suggested the involvement of neurons involved in ER stress. Several apoptosis mediators are implicated in ER stress-associated cell death such as GRP78, CHOP, and the activation of ER-associated caspase-12[37]. CHOP, known as DNA damage-inducible gene 153, is a major pro-apoptotic factor activated by ER stress and plays a critical role in the process of apoptosis[38]. In our study, we found that the ER stress markers (GRP78), three sensors (PERK, IRE1α, ATF6) (Fig. 5), and downstream molecule (CHOP) were all statistically significant upregulated after SCIRI (Fig. 6). Our results confirmed that SCIRI induces the activation of ER stress, which led to the high expression of CHOP. More importantly, we found that Xe postconditioning weakened the expression of ER stress-related proteins, including the above-mentioned proteins. Administration of 4-PBA significantly inhibited expression of CHOP, further demonstrating that Xe postconditioning may protect the spinal cord by inhibiting the ER stress pathway.

Bcl-2, an anti-apoptotic protein, can decrease mitochondrial permeability and inhibit apoptosis, whereas Bax, a pro-apoptotic protein, accelerates apoptosis by increasing mitochondrial permeability and the release of cytochrome c[39]. ER stress-induced in mitochondria released cytochrome C into the cytosol, which further activated caspase-3 and caspase-9. ER stress-induced activation of caspase-3 dissociates procaspase-12 from the ER membrane, finally evoking the caspase-cascade reaction and leading to cell apoptosis[40, 41]. Evidence obtained in recent years has demonstrated that ER-mediated cell death plays an important role in the mechanisms underlying I/R neuronal damage. CHOP is activated by PERK and ATF6, which induces apoptosis by repressing the expression of the anti-apoptotic protein Bcl-2 and upregulating of pro-apoptotic protein Bax[42]. A previous study demonstrated that Xe exerts its neuroprotective effect by regulating Bcl-2/Bax and reducing apoptosis[22], which is consistent with our experimental results. In this study, we demonstrated that ER stress-induced apoptosis was involved in the responses of SCIRI, and the levels of related proteins including GRP78, CHOP, caspase-3 protein and the rate of Bax/Bcl-2 clearly increased (Fig. 6). Xe postconditioning significantly decreased expression of the above-mentioned proteins, suggesting that the neuroprotective effect of Xe was related to the inhibition of ER stress-induced apoptosis. To further verify whether the neuroprotective effect of Xe against SCIRI is mediated by inhibition of ER stress-induced apoptosis, 4-PBA (an ER stress inhibitor) was applied in this study. When pretreated with 4-PBA, the number of apoptotic cells, expression of caspase-3 proteins, and rate of Bax/Bcl-2 were decreased. Meanwhile, a significant anti-apoptotic effect of 4-PBA was also observed. However, in the presence of 4-PBA, Xe did not further enhance the anti-ER stress effect,

indicating that both Xe and 4-PBA induced anti-ER stress effects mediated by the same mechanism. Although Xe further enhanced the anti-apoptotic effect on the spinal cord after co-treatment with 4-PBA, the degree was less than that of Xe treatment, suggesting that the neuroprotection of Xe was partially by inhibiting ER stress-mediated apoptosis.

Combined with the above experimental results, this study had several limitations. First, animals were sacrificed at 4 h after reperfusion; therefore, the long-term effects of Xe could not be detected, which may be an important variable in determining spinal cord survival after IRI. Second, we found that UPR mediated three main signaling branches: IRE1α, PERK, and ATF6, and was not involved in subsequent specific signaling pathways, whereas several pathways are involved in ER stress-autophagy pathways, which may also be involved in Xe-induced neuroprotection. Third, our study focused only on neuronal damage following SCIRI, while microglia and astrocytes play important roles in the inflammatory response after SCIRI. Therefore, we will continue to study the mechanism of neuronal apoptosis to accelerate rehabilitation after IRI.

In conclusion, we speculate that the ER stress-induced neuronal apoptosis participates in the pathogenesis of SCIRI, and Xe postconditioning protects tissues from SCIRI by inhibiting this pathway.

Declarations

Acknowledgements

We thank LetPub (www.letpub.com) for its linguistic assistance during the preparation of this manuscript.

Author contributions

Study design and conception: Mu Jin; experiment implementation and data collection: Lan Luo, Yuqing Wang, Jiaqi Tong, Lu Li, Yanbing Zhu; data analysis: Lan Luo and Mu Jin; manuscript draft: Lan Luo and Mu Jin. Lan Luo and Yuqing Wang contributed equally to this work. All authors read and approved the final manuscript.

Funding

This work was supported by the Natural Science Foundation of Beijing Municipality (Grant 7192047).

Disclosure statement

The authors declare no conflicts of interest.

References

1. Gaudino M, Khan FM, Rahouma M, Naik A, Hameed I, Spadaccio C, Robinson NB, Ruan Y, Demetres M, Oakley CT, Gambardella I, Iannacone EM, Lau C, Girardi LN (2022) Spinal cord injury after open and endovascular repair of descending thoracic and thoracoabdominal aortic aneurysms: A meta-analysis. J Thorac Cardiovasc Surg 163(2):552-564 https://doi.org/10.1016/j.jtcvs.2020.04.126
2. Tenorio ER, Oderich GS, Farber MA, Schneider DB, Timaran CH, Schanzer A, Beck AW, Motta F, Sweet MP, Fenestrated US, Branched Aortic Research Consortium I (2020) Outcomes of endovascular repair of chronic postdissection compared with degenerative thoracoabdominal aortic aneurysms using fenestrated-branched stent grafts. J Vasc Surg 72(3):822-836 e829 https://doi.org/10.1016/j.jvs.2019.10.091
3. Hou J, Li H, Xue C, Ma J (2022) Lidocaine relieves spinal cord ischemia-reperfusion injury via long non-coding RNA MIAT-mediated Notch1 downregulation. J Biochem 171(4):411-420 https://doi.org/10.1093/jb/mvab150
4. Jing N, Fang B, Li Z, Tian A (2020) Exogenous activation of cannabinoid-2 receptor modulates TLR4/MMP9 expression in a spinal cord ischemia reperfusion rat model. J Neuroinflammation 17(1):101 https://doi.org/10.1186/s12974-020-01784-7
5. Rong Y, Fan J, Ji C, Wang Z, Ge X, Wang J, Ye W, Yin G, Cai W, Liu W (2022) USP11 regulates autophagy-dependent ferroptosis after spinal cord ischemia-reperfusion injury by deubiquitinating Beclin 1. Cell Death Differ 29(6):1164-1175 https://doi.org/10.1038/s41418-021-00907-8
6. Li Q, Gao S, Kang Z, Zhang M, Zhao X, Zhai Y, Huang J, Yang GY, Sun W, Wang J (2018) Rapamycin Enhances Mitophagy and Attenuates Apoptosis After Spinal Ischemia-Reperfusion Injury. Front Neurosci 12:865 https://doi.org/10.3389/fnins.2018.00865
7. Li Y, Lin S, Xu C, Zhang P, Mei X (2018) Triggering of Autophagy by Baicalein in Response to Apoptosis after Spinal Cord Injury: Possible Involvement of the PI3K Activation. Biol Pharm Bull 41(4):478-486 https://doi.org/10.1248/bpb.b17-00768
8. Gu C, Li L, Huang Y, Qian D, Liu W, Zhang C, Luo Y, Zhou Z, Kong F, Zhao X, Liu H, Gao P, Chen J, Yin G (2020) Salidroside Ameliorates Mitochondria-Dependent Neuronal Apoptosis after Spinal Cord Ischemia-Reperfusion Injury Partially through Inhibiting Oxidative Stress and Promoting Mitophagy. Oxid Med Cell Longev 2020:3549704 https://doi.org/10.1155/2020/3549704
9. Lu X, Lv C, Zhao Y, Wang Y, Li Y, Ji C, Wang Z, Ye W, Yu S, Bai J, Cai W (2022) TSG-6 released from adipose stem cells-derived small extracellular vesicle protects against spinal cord ischemia reperfusion injury by inhibiting endoplasmic reticulum stress. Stem Cell Res Ther 13(1):291 https://doi.org/10.1186/s13287-022-02963-4
10. Chen X, Cubillos-Ruiz JR (2021) Endoplasmic reticulum stress signals in the tumour and its microenvironment. Nat Rev Cancer 21(2):71-88 https://doi.org/10.1038/s41568-020-00312-2
11. Hu H, Tian M, Ding C, Yu S (2018) The C/EBP Homologous Protein (CHOP) Transcription Factor Functions in Endoplasmic Reticulum Stress-Induced Apoptosis and Microbial Infection. Front Immunol 9:3083 https://doi.org/10.3389/fimmu.2018.03083

12. Kong FJ, Ma LL, Guo JJ, Xu LH, Li Y, Qu S (2018) Endoplasmic reticulum stress/autophagy pathway is involved in diabetes-induced neuronal apoptosis and cognitive decline in mice. Clin Sci (Lond) 132(1):111-125 https://doi.org/10.1042/CS20171432
13. Xu L, Bi Y, Xu Y, Wu Y, Du X, Mou Y, Chen J (2021) Suppression of CHOP Reduces Neuronal Apoptosis and Rescues Cognitive Impairment Induced by Intermittent Hypoxia by Inhibiting Bax and Bak Activation. Neural Plast 2021:4090441 https://doi.org/10.1155/2021/4090441
14. Wu C, Xu H, Li J, Hu X, Wang X, Huang Y, Li Y, Sheng S, Wang Y, Xu H, Ni W, Zhou K (2020) Baicalein Attenuates Pyroptosis and Endoplasmic Reticulum Stress Following Spinal Cord Ischemia-Reperfusion Injury via Autophagy Enhancement. Front Pharmacol 11:1076 https://doi.org/10.3389/fphar.2020.01076
15. Jin Z, Piazza O, Ma D, Scarpati G, De Robertis E (2019) Xenon anesthesia and beyond: pros and cons. Minerva Anestesiol 85(1):83-89 https://doi.org/10.23736/S0375-9393.18.12909-9
16. Campos-Pires R, Onggradito H, Ujvari E, Karimi S, Valeo F, Aldhoun J, Edge CJ, Franks NP, Dickinson R (2020) Xenon treatment after severe traumatic brain injury improves locomotor outcome, reduces acute neuronal loss and enhances early beneficial neuroinflammation: a randomized, blinded, controlled animal study. Crit Care 24(1):667 https://doi.org/10.1186/s13054-020-03373-9
17. Liang M, Ahmad F, Dickinson R (2022) Neuroprotection by the noble gases argon and xenon as treatments for acquired brain injury: a preclinical systematic review and meta-analysis. Br J Anaesth 129(2):200-218 https://doi.org/10.1016/j.bja.2022.04.016
18. De Deken J, Rex S, Monbaliu D, Pirenne J, Jochmans I (2016) The Efficacy of Noble Gases in the Attenuation of Ischemia Reperfusion Injury: A Systematic Review and Meta-Analyses. Crit Care Med 44(9):e886-896 https://doi.org/10.1097/CCM.0000000000001717
19. Ma D, Lim T, Xu J, Tang H, Wan Y, Zhao H, Hossain M, Maxwell PH, Maze M (2009) Xenon preconditioning protects against renal ischemic-reperfusion injury via HIF-1alpha activation. J Am Soc Nephrol 20(4):713-720 https://doi.org/10.1681/ASN.2008070712
20. Stoppe C, Ney J, Brenke M, Goetzenich A, Emontzpohl C, Schalte G, Grottke O, Moeller M, Rossaint R, Coburn M (2016) Sub-anesthetic Xenon Increases Erythropoietin Levels in Humans: A Randomized Controlled Trial. Sports Med 46(11):1753-1766 https://doi.org/10.1007/s40279-016-0505-1
21. Liu S, Yang Y, Jin M, Hou S, Dong X, Lu J, Cheng W (2016) Xenon-delayed postconditioning attenuates spinal cord ischemia/reperfusion injury through activation AKT and ERK signaling pathways in rats. J Neurol Sci 368:277-284 https://doi.org/10.1016/j.jns.2016.07.009
22. Yang YW, Wang YL, Lu JK, Tian L, Jin M, Cheng WP (2018) Delayed xenon post-conditioning mitigates spinal cord ischemia/reperfusion injury in rabbits by regulating microglial activation and inflammatory factors. Neural Regen Res 13(3):510-517 https://doi.org/10.4103/1673-5374.228757
23. Fang H, Yang M, Pan Q, Jin HL, Li HF, Wang RR, Wang QY, Zhang JP (2021) MicroRNA-22-3p alleviates spinal cord ischemia/reperfusion injury by modulating M2 macrophage polarization via IRF5. J Neurochem 156(1):106-120 https://doi.org/10.1111/jnc.15042

24. You YD, Deng WH, Guo WY, Zhao L, Mei FC, Hong YP, Zhou Y, Yu J, Xu S, Wang WX (2019) 4-Phenylbutyric Acid Attenuates Endoplasmic Reticulum Stress-Mediated Intestinal Epithelial Cell Apoptosis in Rats with Severe Acute Pancreatitis. Dig Dis Sci 64(6):1535-1547 https://doi.org/10.1007/s10620-018-5437-1
25. Hong YP, Deng WH, Guo WY, Shi Q, Zhao L, You YD, Mei FC, Zhou Y, Wang CY, Chen C, Yu J, Wang WX (2018) Inhibition of endoplasmic reticulum stress by 4-phenylbutyric acid prevents vital organ injury in rat acute pancreatitis. Am J Physiol Gastrointest Liver Physiol 315(5):G838-G847 https://doi.org/10.1152/ajpgi.00102.2018
26. Sun F, Zhang H, Shi J, Huang T, Wang Y (2021) Astragalin Protects against Spinal Cord Ischemia Reperfusion Injury through Attenuating Oxidative Stress-Induced Necroptosis. Biomed Res Int 2021:7254708 https://doi.org/10.1155/2021/7254708
27. Zhao L, Zhai M, Yang X, Guo H, Cao Y, Wang D, Li P, Liu C (2019) Dexmedetomidine attenuates neuronal injury after spinal cord ischaemia-reperfusion injury by targeting the CNPY2-endoplasmic reticulum stress signalling. J Cell Mol Med 23(12):8173-8183 https://doi.org/10.1111/jcmm.14688
28. Fu J, Sun H, Wei H, Dong M, Zhang Y, Xu W, Fang Y, Zhao J (2020) Astaxanthin alleviates spinal cord ischemia-reperfusion injury via activation of PI3K/Akt/GSK-3beta pathway in rats. J Orthop Surg Res 15(1):275 https://doi.org/10.1186/s13018-020-01790-8
29. Veldeman M, Coburn M, Rossaint R, Clusmann H, Nolte K, Kremer B, Hollig A (2017) Xenon Reduces Neuronal Hippocampal Damage and Alters the Pattern of Microglial Activation after Experimental Subarachnoid Hemorrhage: A Randomized Controlled Animal Trial. Front Neurol 8:511 https://doi.org/10.3389/fneur.2017.00511
30. Liu F, Liu S, Patterson TA, Fogle C, Hanig JP, Slikker W, Jr., Wang C (2020) Effects of Xenon-Based Anesthetic Exposure on the Expression Levels of Polysialic Acid Neural Cell Adhesion Molecule (PSA-NCAM) on Human Neural Stem Cell-Derived Neurons. Mol Neurobiol 57(1):217-225 https://doi.org/10.1007/s12035-019-01771-x
31. Yang YW, Lu JK, Qing EM, Dong XH, Wang CB, Zhang J, Zhao LY, Gao ZF, Cheng WP (2012) Post-conditioning by xenon reduces ischaemia-reperfusion injury of the spinal cord in rats. Acta Anaesthesiol Scand 56(10):1325-1331 https://doi.org/10.1111/j.1399-6576.2012.02718.x
32. Zhang Y, Zhang M, Liu S, Zhu W, Yu J, Cui Y, Pan X, Gao X, Wang Q, Sun H (2019) Xenon exerts anti-seizure and neuroprotective effects in kainic acid-induced status epilepticus and neonatal hypoxia-induced seizure. Exp Neurol 322:113054 https://doi.org/10.1016/j.expneurol.2019.113054
33. Ren J, Bi Y, Sowers JR, Hetz C, Zhang Y (2021) Endoplasmic reticulum stress and unfolded protein response in cardiovascular diseases. Nat Rev Cardiol 18(7):499-521 https://doi.org/10.1038/s41569-021-00511-w
34. Zhang S, Yan Y, Wang Y, Sun Z, Han C, Qian X, Ren X, Feng Y, Cai J, Xia C (2021) Inhibition of MALT1 Alleviates Spinal Ischemia/Reperfusion Injury-Induced Neuroinflammation by Modulating Glial Endoplasmic Reticulum Stress in Rats. J Inflamm Res 14:4329-4345 https://doi.org/10.2147/JIR.S319023

35. Zhao J, Wang L, Li Y (2017) Electroacupuncture Alleviates the Inflammatory Response via Effects on M1 and M2 Macrophages after Spinal Cord Injury. Acupuncture in Medicine 35(3):224-230 https://doi.org/10.1136/acupmed-2016-011107
36. Chen Z, Guo H, Lu Z, Sun K, Jin Q (2019) Hyperglycemia aggravates spinal cord injury through endoplasmic reticulum stress mediated neuronal apoptosis, gliosis and activation. Biomed Pharmacother 112:108672 https://doi.org/10.1016/j.biopha.2019.108672
37. Zhu H, Zhou H (2021) Novel Insight into the Role of Endoplasmic Reticulum Stress in the Pathogenesis of Myocardial Ischemia-Reperfusion Injury. Oxid Med Cell Longev 2021:5529810 https://doi.org/10.1155/2021/5529810
38. Li CF, Pan YK, Gao Y, Shi F, Wang YC, Sun XQ (2019) Autophagy protects HUVECs against ER stress-mediated apoptosis under simulated microgravity. Apoptosis 24(9-10):812-825 https://doi.org/10.1007/s10495-019-01560-w
39. Carpio MA, Michaud M, Zhou W, Fisher JK, Walensky LD, Katz SG (2015) BCL-2 family member BOK promotes apoptosis in response to endoplasmic reticulum stress. Proceedings of the National Academy of Sciences 112(23):7201-7206 https://doi.org/10.1073/pnas.1421063112
40. Tian Y, Wang L, Qiu Z, Xu Y, Hua R (2021) Autophagy triggers endoplasmic reticulum stress and C/EBP homologous protein-mediated apoptosis in OGD/R-treated neurons in a caspase-12-independent manner. J Neurophysiol 126(5):1740-1750 https://doi.org/10.1152/jn.00649.2020
41. He Q, Wang T, Ni H, Liu Q, An K, Tao J, Chen Y, Xu L, Zhu C, Yao M (2019) Endoplasmic reticulum stress promoting caspase signaling pathway-dependent apoptosis contributes to bone cancer pain in the spinal dorsal horn. Mol Pain 15:1744806919876150 https://doi.org/10.1177/1744806919876150
42. Zhang M, Du H, Huang Z, Zhang P, Yue Y, Wang W, Liu W, Zeng J, Ma J, Chen G, Wang X, Fan J (2018) Thymoquinone induces apoptosis in bladder cancer cell via endoplasmic reticulum stress-dependent mitochondrial pathway. Chem Biol Interact 292:65-75 https://doi.org/10.1016/j.cbi.2018.06.013

Tables

Table 1 Primer sequences for RT-PCR

Primer	Forward 5'–3'	Reverse 5'–3'
GRP78	CACTTGGTATTGAAACTGTGGG	TGTTACGGTGGGCTGATTAT
ATF6	GCAGGTGTATTACGCTTCG	TTCGGTCTTGTGGTCTTGTT
IRE1α	GACGAGCATCCGAATGTGATCCG	GAGGTGGTCTGATGAAGCAAGGTG
PERK	TGGTAAAGTCATCCCCATCAGTC	CCTTGTAGGGAACTTTTCCA
CHOP	CTGAAGAGAACGAGCGGCTCAAG	GACAGGTGATGCCAACAGTTC
Bax	CCCGAGAGGTCTTCTTCC	GAAGTCCAGTGTCCAGCCCA
Bcl-2	GTGAACTGGGGGAGGATTGT	GCATCCCAGCCTCCGTTA
Caspase-3	CGGACCTGTGGACCTGAAAA	TTCCACTGTCTGTCTCAATACCG
β-actin	GGAGATTACTGCCCTGGCTCCTA	GACTCATCGTACTCCTGCTTGCTG

Figures

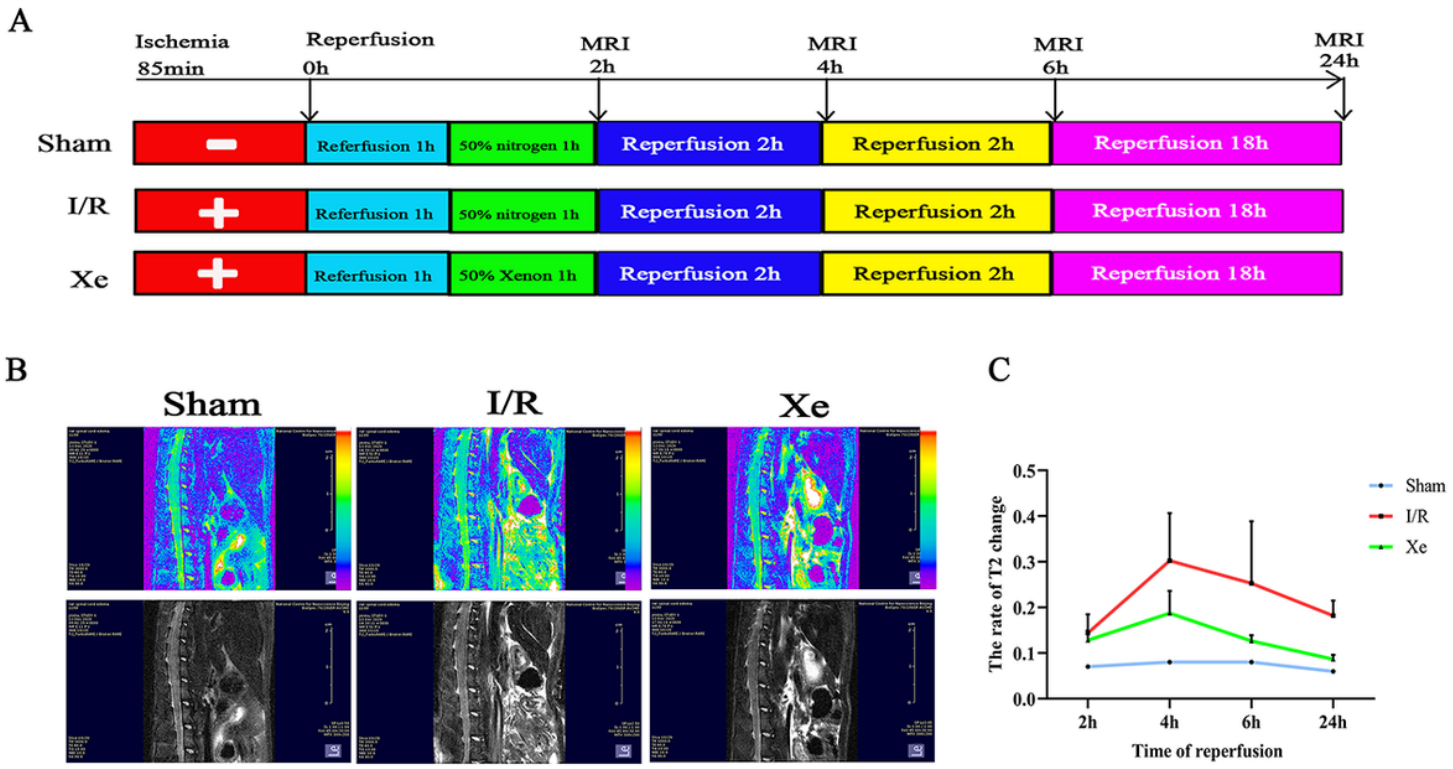

Figure 1

Protocol for experiment 1 and magnetic resonance imaging of the lumbar spinal cord. (A) Protocol for experiment 1. (B) Magnetic resonance imaging of the lumbar spinal cord at 4h after SCIRI. The spinal edema imaging sequence was T2_TurboRARE sequence, and the parameters were as follows: Number of slices=20, TR=000ms, TE=40ms, matrix=300×200, FOV=45×30mm, flip Angle=90 and slice

thickness=1mm, ETL=10, NEX=10. Splashing sequence T2map_MESE was adopted for T2 imaging of the spinal cord, with the following parameters: Number of slices=20, TR=3000ms, TE=6.6/13.2/...72.6/79.2ms, matrix=150×100, FOV=45×30mm, Flip Angle=90 and slice thickness=1mm, ETL=1, NEX =1. T2 values of spinal cord were obtained by curve fitting of T2 imaging signal intensity with multiple echo time using Levenberg-Marquardt algorithm. (C) The rate of T2 change at 2, 4, 6 and 24 h after reperfusion.

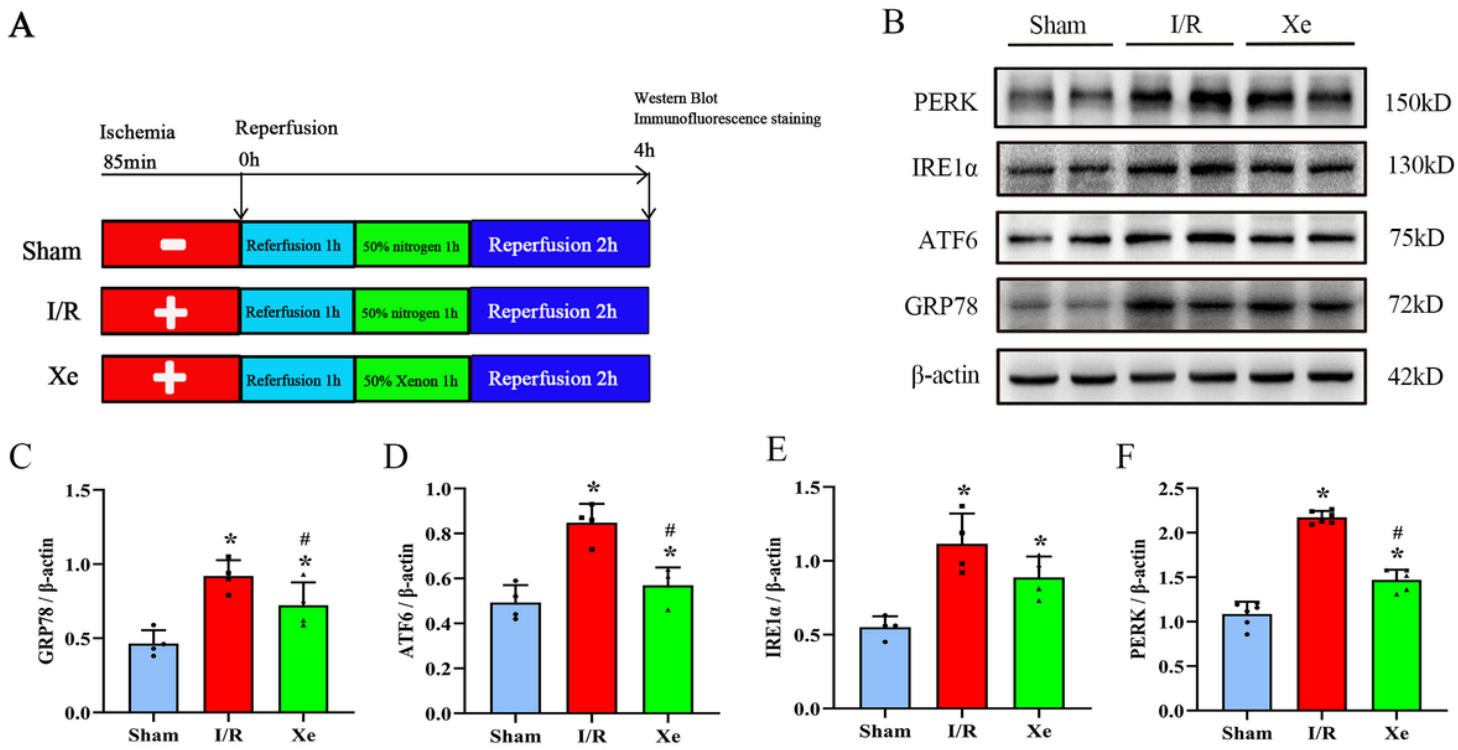

Figure 2

Protocol for experiment 2 and the effect of xenon postconditioning on ER stress related protein expression in rats with SCIRI, as detected by western blot. (A) Protocol for experiment 2. (B) Representative Western blots showing the changes in the expression of GRP78, IRE1α, ATF6 and PERK. (C-F) Expression levels of GRP78, IRE1α, ATF6 and PERK in the spinal cord were normalized to β-actin levels within the same sample. All data are presented as the mean ± SD, n=5, $^{*}P<0.05$ vs Sham, $^{\#}P<0.05$ vs I/R.

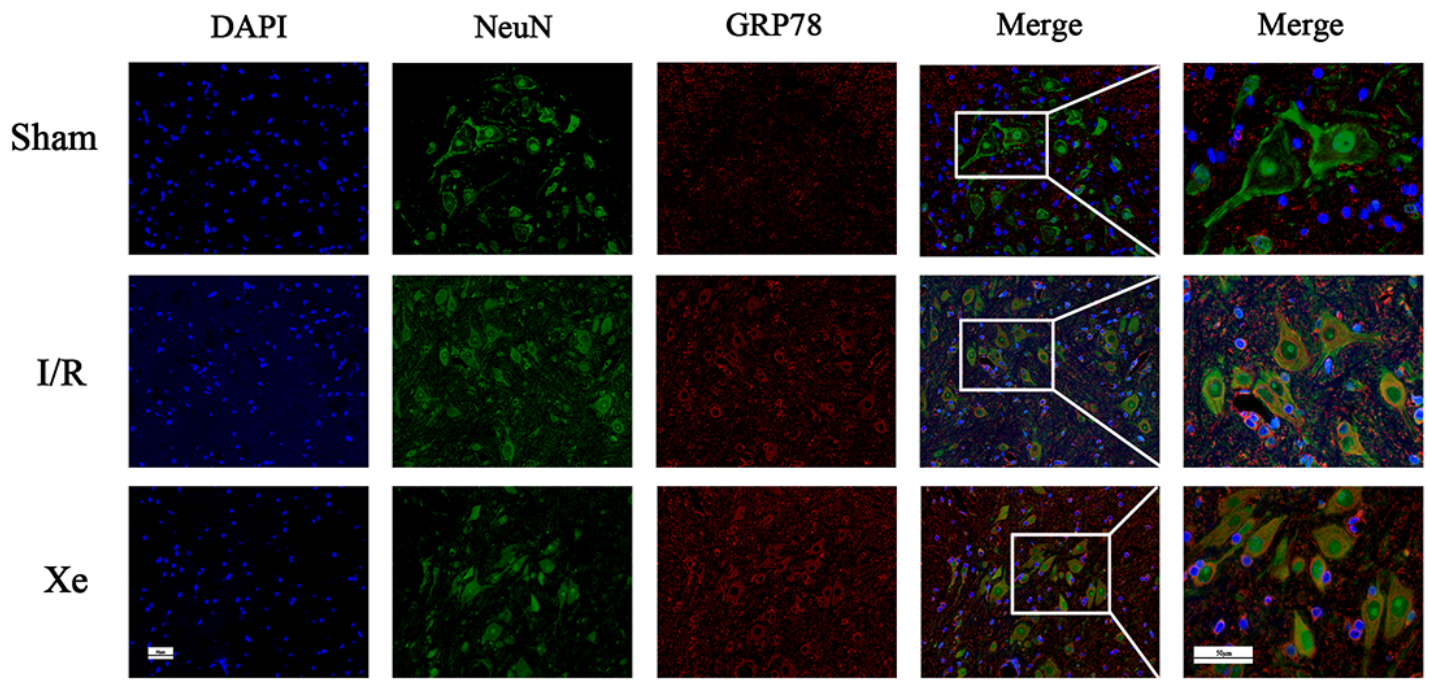

Figure 3

Representative co-staining images with GRP8 and NeuN captured at spinal cord after SCIRI. Scale bar = 50 μm.

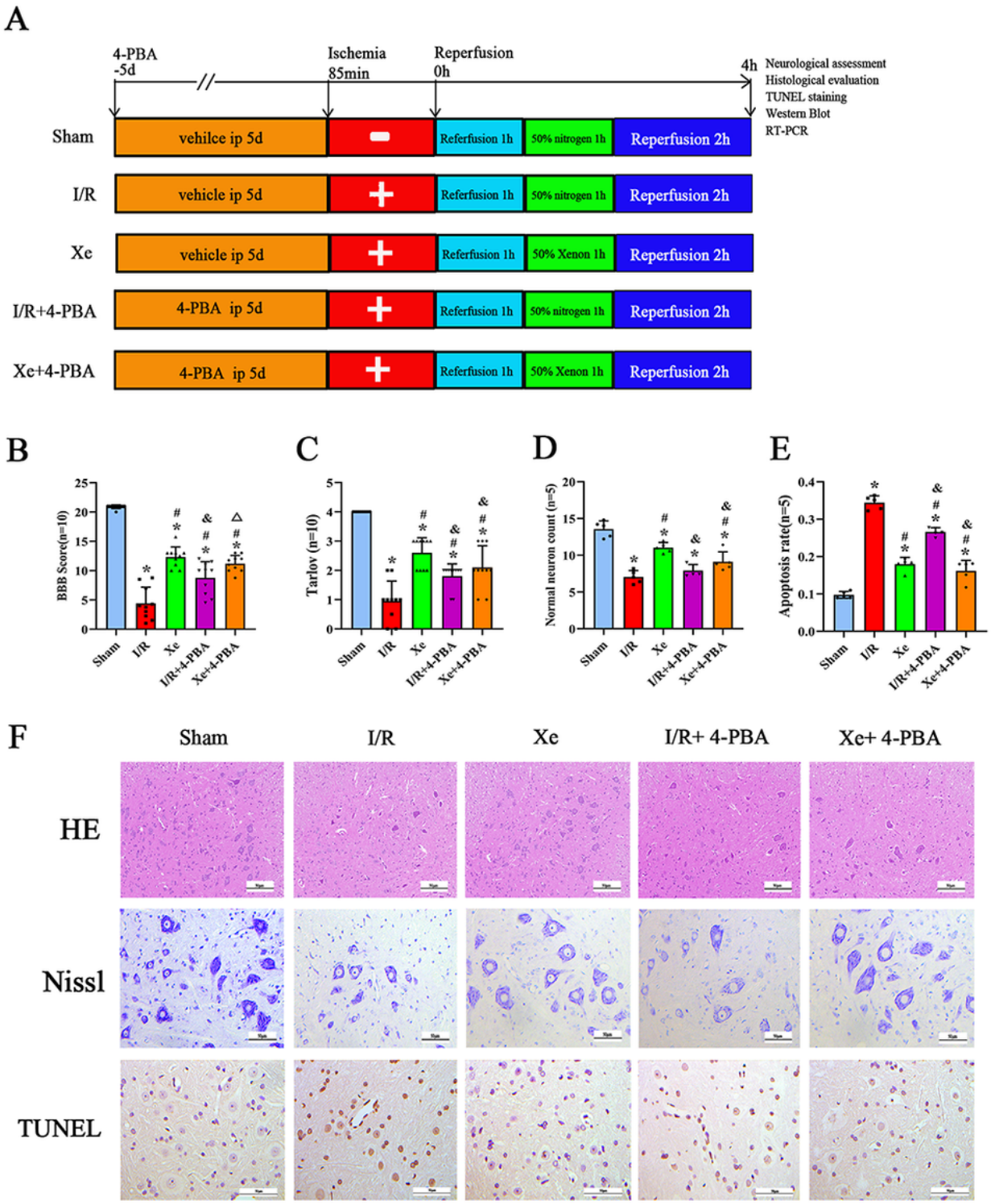

Figure 4

Protocol for experiment 3 and the effect of xenon post-conditioning on motor function, histopathologic change and neuron apoptosis in rats with SCIRI. (A) Protocol for experiment 3. (B) BBB open-field locomotor scales after SCIRI. (C) Tarlov score after SCIRI. (D) The count of normal neurons in spinal cord. (E) Neural cell apoptosis rate in the rat spinal cord tissue. (F) Representative image of Hematoxylin-eosin (H&E) staining, Nissl staining and TUNEL staining of the spinal cord tissues. All data are presented as the

mean ± SD, n=5, Scale bar = 50 μm, $^{*}P$<0.05 vs Sham, $^{\#}P$<0.05 vs I/R, $^{\&}P$<0.05 vs Xe, $^{\triangle}P$<0.05 vs I/R+4-PBA.

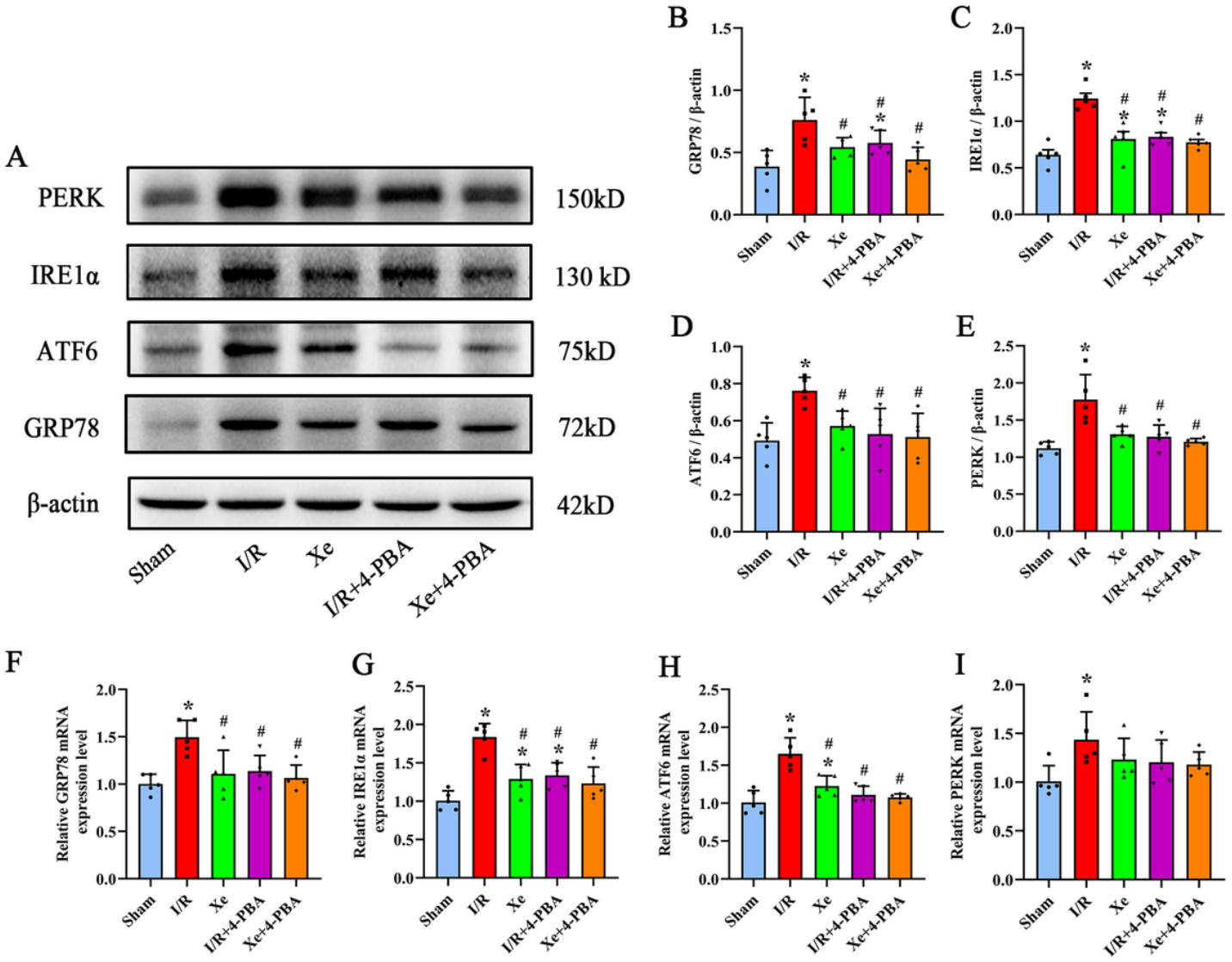

Figure 5

Effect of xenon postconditioning on the ER stress related protein expression in rats with SCIRI, as detected by western blot and Real-Time PCR. (A) Representative Western blots showing the changes in the expression of GRP78, IRE1α, ATF6 and PERK. (B-E) Expression levels of GRP78, IRE1α, ATF6 and PERK in the spinal cord were normalized to β-actin levels within the same sample. (F-I) Relative expression of GRP78, IRE1α, ATF6 and PERK mRNA in the spinal cord of each group. All data are presented as the mean ± SD, n=5, $^{*}P$<0.05 vs Sham, $^{\#}P$<0.05 vs I/R.

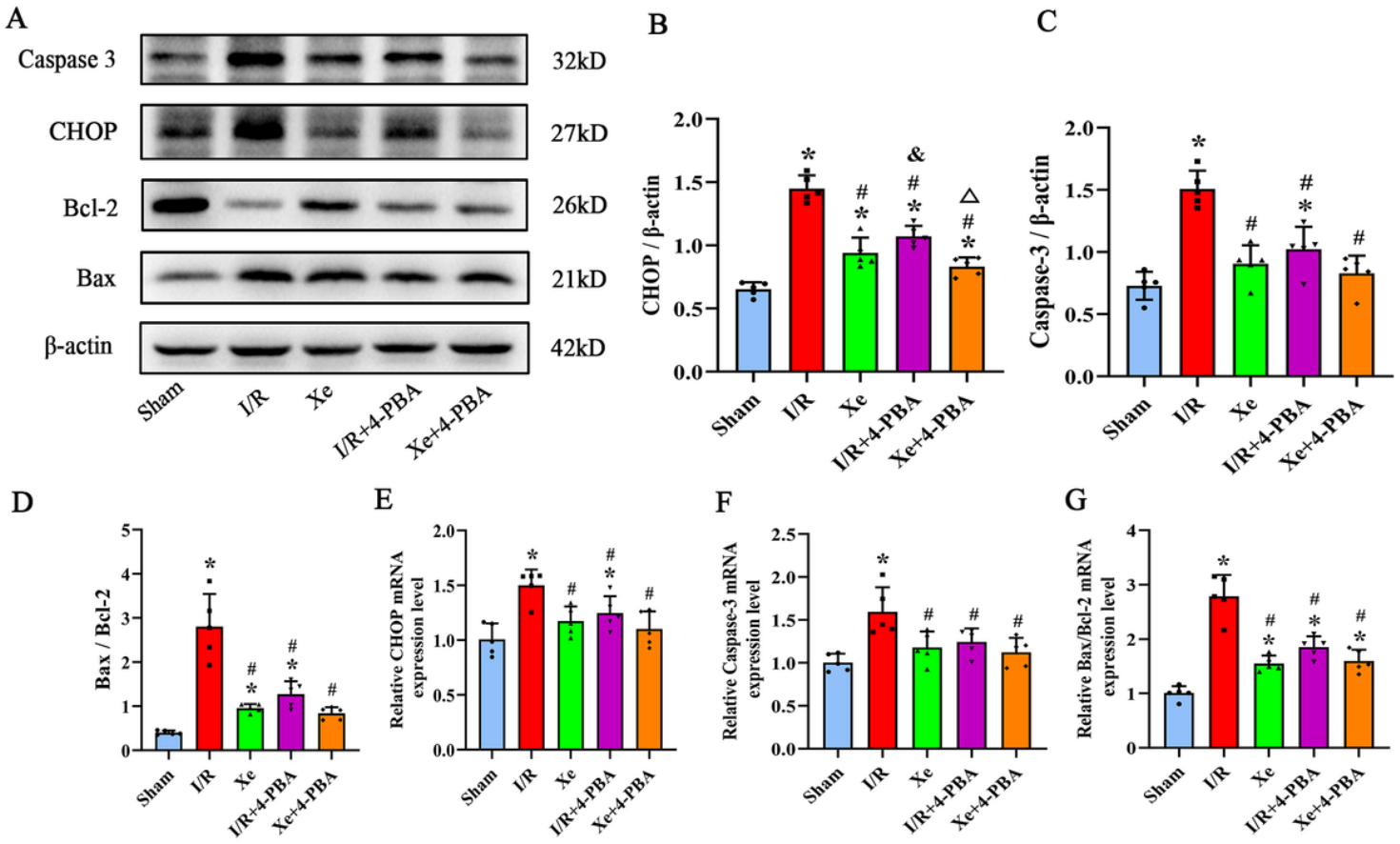

Figure 6

Effect of xenon postconditioning on the ER stress related apoptosis protein expression in rats after SCIRI, as detected by western blot and Real-Time PCR. (A-D) Representative Western blots showing the changes in the expression of CHOP, Caspasse-3, Bcl-2, Bax. (E-G) Relative expression of CHOP, Caspasse-3, Bcl-2, Bax mRNA in the spinal cord of each group. All data are presented as the mean ± SD, n=5, $^{*}P<0.05$ vs Sham, $^{\#}P<0.05$ vs I/R, $^{\&}P<0.05$ vs Xe, $^{\triangle}P<0.05$ vs I/R+4-PBA.